

UC San Diego

UC San Diego Previously Published Works

Title

Abrupt Change in Forest Height along a Tropical Elevation Gradient Detected Using Airborne Lidar

Permalink

<https://escholarship.org/uc/item/02x8j8pk>

Journal

Remote Sensing, 8(10)

ISSN

2072-4292

Authors

Wolf, Jeffrey
Brocard, Gilles
Willenbring, Jane
et al.

Publication Date

2016

DOI

10.3390/rs8100864

Peer reviewed

1 *Communication*

2 **Abrupt change in forest height along a tropical** 3 **elevation gradient detected using airborne lidar**

4 **Jeffrey Wolf** ^{1,*}, **Gilles Brocard** ², **Jane Willenbring** ², **Stephen Porder** ³ and **Maria Uriarte** ¹

5 ¹ Department of Ecology, Evolution and Environmental Biology, Columbia University, New York, NY;
6 iamjwolf@gmail.com, mu2126@columbia.edu

7 ² Department of Earth and Environmental Sciences, University of Pennsylvania, Philadelphia, PA;
8 gilles.brocard@sydney.edu.au, erosion@sas.upenn.edu

9 ³ Department of Ecology and Evolutionary Biology, Brown University, Providence, RI;
10 stephen_porder@brown.edu

11 * Correspondence: iamjwolf@gmail.com

12 Academic Editor: name

13 Received: date; Accepted: date; Published: date

14 **Abstract:** Most research on vegetation in mountain ranges focuses on elevation gradients as climate
15 gradients, but elevation gradients are also the result of geological processes that build and
16 deconstruct mountains. Recent findings from the Luquillo Mountains, Puerto Rico, have raised
17 questions about whether erosion rates that vary due to past tectonic events and are spatially
18 patterned in relation to elevation may drive vegetation patterns along elevation gradients. Here we
19 use airborne light detection and ranging (lidar) technology to observe forest height over the Luquillo
20 Mountain Range. We show that models with different functional forms for the two prominent
21 bedrock types best describe the forest height - elevation patterns. On one bedrock type there are
22 abrupt decreases in forest height with elevation approximated by a sigmoidal function, with the
23 inflection point near the elevation of where other studies have shown there to be a sharp change in
24 erosion rates triggered by a tectonic uplift event that began approximately 4.2 My ago. Our findings
25 are consistent with broad geologically mediated vegetation patterns along the elevation gradient,
26 consistent with a role for mountain building and deconstructing processes.

27 **Keywords:** ecology; vegetation; geology; active remote sensing; erosion; tectonics; ¹⁰Be; critical zone
28 observatory; long-term ecological research; three-dimensional structure.

29 **PACS:** J0101

30 **1. Introduction**

31 *1.1. Aims*

32 Mountain ranges are often used as ecological laboratories for climate change research [1-3], but
33 elevation gradients are also the result of tectonics and erosion. Erosion rates are important correlates
34 of variation in vegetation cover in mountainous landscapes [4,5]. Differences in erosion patterns can
35 produce soil heterogeneity that influences spatial patterns of vegetation [5]. However, disentangling
36 the relationships between erosion rates and plants requires understanding the root cause of variation
37 in erosion rates. Here we examine vegetation patterns on a tropical elevation gradient where spatial
38 patterns of erosion rates have been directly linked to tectonic uplift history [6,7], providing a novel
39 scenario for understanding vegetation spatial patterns on a tropical elevation gradient.

40 *1.2. Vegetation Observations*

41 Airborne light detection and ranging (lidar) is the state-of-the-art method for observing three-
42 dimensional structural properties of forests at landscape spatial scales [8]. Of all vegetation metrics
43 that can be derived from lidar datasets, maximum height of first returns (e.g. forest height) can be
44 derived most consistently across sensor systems [9]. Forest height is also considered a key
45 ecosystem variable for earth observation [10]. Within sensors systems, forest height correlates
46 strongly with other vegetation metrics such as relative heights (e.g. RH50) and metrics describing
47 the shape of the point cloud or waveform such as the height of maximum laser return density (or
48 height of maximum laser energy) [e.g. 9]. We used lidar-derived forest height to study vegetation
49 patterns at landscape scales in a tropical mountain range.

50 *1.3. Tectonic Uplift and Erosion*

51 The Caribbean Plate underwent tilting approximately 4.2 My ago resulting in the conversion of
52 low elevation islands into high mountaintops [11]. Studies of platform surfaces across Puerto Rico
53 suggest contemporary Puerto Rico was once a paleoisland chain much like the modern Virgin
54 Islands. One platform occurs in the Luquillo Mountains, Puerto Rico [6]. The platform is likely the
55 remnant of a paleoisland, “El Yunque Island”, with the paleoshoreline near 600 m elevation [6-7].

56 The platform is most prominently visible on one of the two main bedrock types, the quartz
57 diorite [6]. Stream longitudinal profiles on the quartz diorite bedrock exhibit sharp changes in
58 gradient, referred to as knickpoints. The knickpoints are clustered at similar elevations across
59 drainage networks. These knickpoints do not coincide with lithological discontinuities, but instead
60 represent the front to an upstream migrating wave of incision that originated at the paleoshoreline
61 [7]. Incision into the surrounding stream slopes has occurred, resulting in steep hillslopes below the
62 knickpoints elevation, but shallow hillslopes above the knickpoints.

63 Spatially explicit measurement of erosion rates has been conducted on the quartz diorite bedrock
64 both above and below the knickpoints using sampling of quartz grains obtained from stream
65 sediments and measurement of the cosmogenic isotope ^{10}Be [6-7]. The concentration of ^{10}Be in quartz
66 grains depends on the duration of time that the quartz grain was near the soil surface and exposed
67 to cosmic rays, so the concentration of ^{10}Be in quartz together with modeling assumptions can be used
68 to estimate erosion rates. When ^{10}Be is measured in quartz grains sampled from stream sediments,
69 erosion rates for catchments, with the output of the catchment at the sampling location, can be
70 estimated. Data on ^{10}Be in quartz grains sampled above and below knickpoints across drainage
71 networks on the quartz diorite indicate that catchment scale erosion rates change abruptly at the
72 knickpoint elevation, where higher erosion rates occur below the knickpoints than above.

73 Because erosion causes removal of surface soils at a higher rate below the knickpoints than
74 above, depth to the saprolite is intimately linked to location on the elevation gradient relative to the
75 knickpoints [6,12]. Soils below the knickpoints are shallow with saprolite replenishing minerals that
76 supply nutrients near the soil surface. In contrast, above the knickpoints the soils are generally deep
77 so minerals from the saprolite are far from the surface. Weatherable minerals (e.g. feldspar) are
78 depleted above the knickpoints on the quartz diorite whereas below the knickpoints soils are rich in
79 weatherable minerals [6]. Cations below the knickpoints are at some of the highest concentrations
80 across the entire mountain range, whereas above the knickpoints cation concentrations of soils are
81 relatively low [9]. The consequence is two soil domains on the quartz diorite governed by erosional
82 patterns set in place by tectonic uplift beginning around 4.2 My ago.

83 *1.4. Additional Information From Stream Longitudinal Profiles*

84 Our analysis is focused on the quartz diorite bedrock type, but we also present results from the
85 other main bedrock type, volcanoclastics. Estimates of erosion rates using cosmogenic isotopes are
86 unavailable for the volcanoclastics. The primary factor preventing estimating erosion rates on the
87 volcanoclastic bedrock is the very low amount of quartz grains in the rock. Because of this, we
88 emphasize the results from the quartz diorite portion of the mountains. However, the stream
89 longitudinal profiles indicate that erosion rates are likely spatially diffuse along the elevation
90 gradient on the volcanoclastic bedrock [6]. Specifically, the elevation of the knickpoints on the quartz

91 diorite represents a zone where catchment scale erosion rates abruptly decrease over a short range of
92 elevations [6-7]. The absence of prominent knickpoints in stream longitudinal profiles on the
93 volcanoclastic bedrocks together with the overall shallower stream longitudinal profiles suggest that
94 erosion rates on the volcanoclastic bedrock are likely more spatially diffuse across the elevation
95 gradient [6]. Specifically, the absence of knickpoints over the same elevations as on the quartz diorite
96 indicates that the wave of incision moved up the mountain more rapidly, likely due to differences in
97 both physical and chemical properties of the volcanoclastic bedrock [6-7,12]. Including the
98 volcanoclastic bedrock may therefore act as a control for forest height – elevation patterns that result
99 primarily from climate variation in relation to elevation.

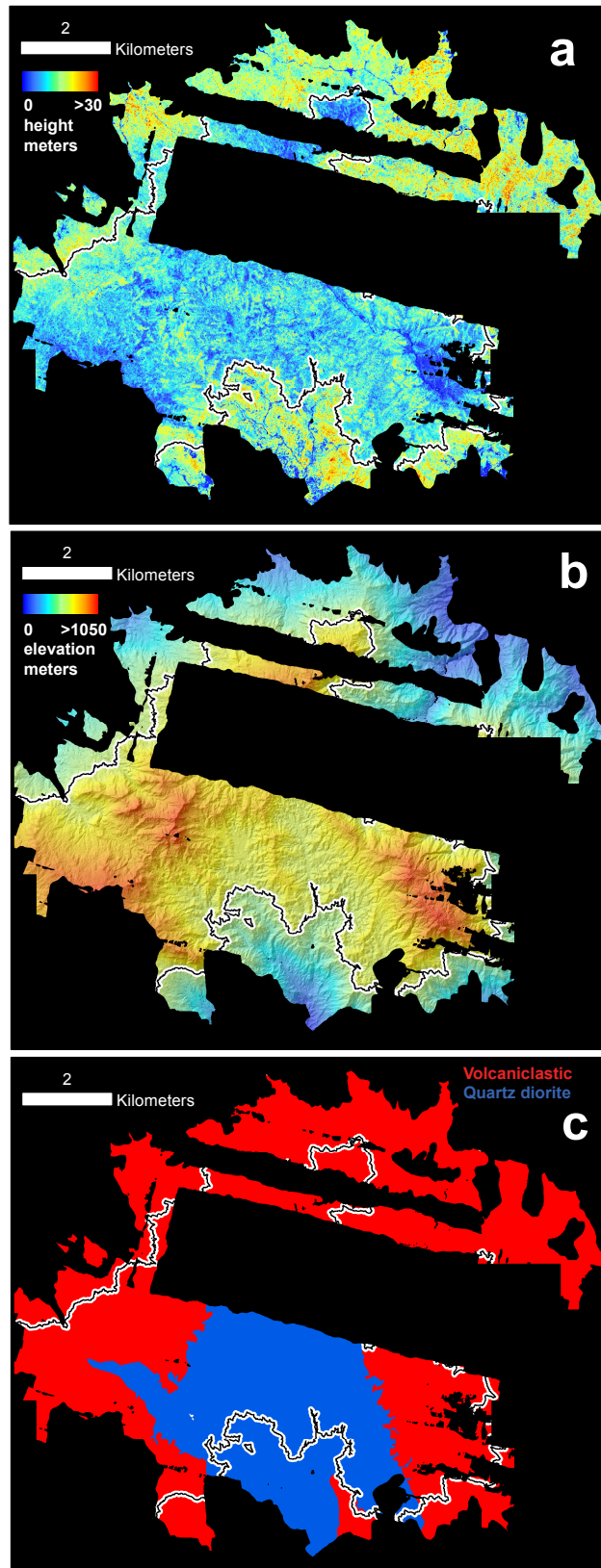
100 1.5. Hypotheses

101 We expected that forest height would decrease abruptly on the quartz diorite bedrock near the
102 elevation of the knickpoints if mountain building and deconstructing processes are important to
103 influencing spatial patterns of vegetation on the elevation gradient. Overall we expected that forest
104 height would decline with increasing elevation on both bedrock types. We expected that since the
105 volcanoclastics lack knickpoints we would not observe abrupt changes in forest height near the same
106 elevation of the quartz diorite knickpoints, regardless of whether or not plants are responding to
107 edaphic (e.g. soil) properties that covary with erosion on the quartz diorite bedrock. Our approach to
108 testing these hypotheses was to consider different functional forms for the forest height - elevation
109 patterns.

110 2. Materials and Methods

111 2.1. Study Area

112 Over a distance of < 20 km, the Luquillo mountains rise from sea level to > 1,050 m elevation.
113 Mean annual precipitation (MAP) ranges from 2,300 mm yr⁻¹ to > 4,500 mm yr⁻¹ and mean annual
114 temperature (MAT) declines from 23°C to 19°C. Geologic maps and field observations were used to
115 assign areas of the landscape to quartz diorite or volcanoclastic bedrock [6-7,12]. The area covered
116 corresponds with the extent of the lidar coverage and area of closed canopy forest since 1936 (based
117 on aerial photographs). Lidar coverage was initially planned for the entire mountain range but due
118 to inclement weather on multiple occasions a central portion of the range was not flown. We focused
119 on the elevation interval of 400 m to 800 m that is centered on the quartz diorite knickpoints elevation
120 of approximately 600 m [6-7]. The elevation interval examined included data for 38.95 km² with 16.31
121 km² on quartz diorite and 22.64 km² on volcanoclastic bedrock. Figure 1 shows a map of the study
122 area.



123
 124
 125
 126
 127
 128

Figure 1. Study Area. (a) Forest height at 1-m² spatial resolution. (b) Elevation at 1-m² spatial resolution. (c) Map of quartz diorite (blue) and volcaniclastic bedrock (red). The black curve underlain by white illustrates the 600 m contour interval representing the approximate elevation of the paleoshoreline and contemporary elevation of the regional knickpoints on quartz diorite. The study area is restricted to portions of the Luquillo Mountains with airborne lidar data and forest cover in 1936.

129 2.2. Dataset

130 Airborne lidar data were collected by the National Center for Airborne Laser Mapping
 131 (NCALM) with an Optech GEMINI ALTM (Telodyne Optech, Ontario, Canada) and Applanix
 132 POS/AV 510 OEM with embedded BD950 12 channel 10 Hz GPS receiver (Applanix Corp., Ontario,
 133 Canada) onboard a Cessna Skymaster (Cessna, Wichita, KS). Data used here are from flights in May
 134 2011. The laser wavelength was 1047 nm, laser pulse frequency was set to 100 Hz, beam divergence
 135 was 0.25 mrad (1/e), scan frequency was set to 55 Hz, scan angle was set to $\pm 15^\circ$, and scan cutoff was
 136 $\pm 2^\circ$. Flights were at an altitude of 600 m and speed of 60 m/s. The swath width was 277.04 m with
 137 50% swath overlap. Point density was approximately 14 points m^{-2} . Discrete-returns were
 138 horizontally referenced to NAD 1983 UTM Zone 20 N (EPSG: 26920) and vertically referenced to
 139 NADV 1988 (EPSG: 5703). Data are available online through OpenTopography
 140 (www.opentopography.org).

141 2.3. Data Processing

142 Discrete laser returns were rasterized at 1- m^2 spatial resolution into a digital surface model
 143 (DSM) and a digital elevation model (DEM). Maximum z-value of the first returns at 1- m^2 spatial
 144 resolution were used for the DSM while minimum z-values of the last-return ground classified
 145 points were used for the DEM. Elevations for DEM pixels without ground returns were estimated
 146 by triangulation of the point cloud. A digital canopy model (DCM) representing forest height was
 147 made by taking the difference of the DSM and DEM. Stand-level height was measured using the 1-
 148 m spatial resolution DCM through averaging all forest height measurements at 1-ha scale.
 149 Resampling was done with Geospatial Data Abstraction Library (GDAL) (www.gdal.org).

150 2.4. Statistical Analysis

151 All datasets were analyzed at the hectare scale resulting in sample sizes of 1631- ha on quartz
 152 diorite and 2264 - ha on volcanoclastic bedrock. Statistical analyses were done using the R Statistical
 153 Computing Environment (R Core Development Team, 2016). Hectare scale data were also aggregated
 154 into 10 m elevation bins to statistically summarize aggregated hectare scale data at discrete elevation
 155 intervals.

156 We tested a series of functional forms to model stand-level forest height in relation to elevation.
 157 We evaluated a linear functional form $H = \beta_0 + \beta_1 x$ (1) and quadratic functional form $H = \beta_0 + \beta_1 x + \beta_2 x^2$
 158 (2) where H is height and β_i is the coefficient for elevation x to the power i ; and sigmoid (logistic)
 159 functional form,

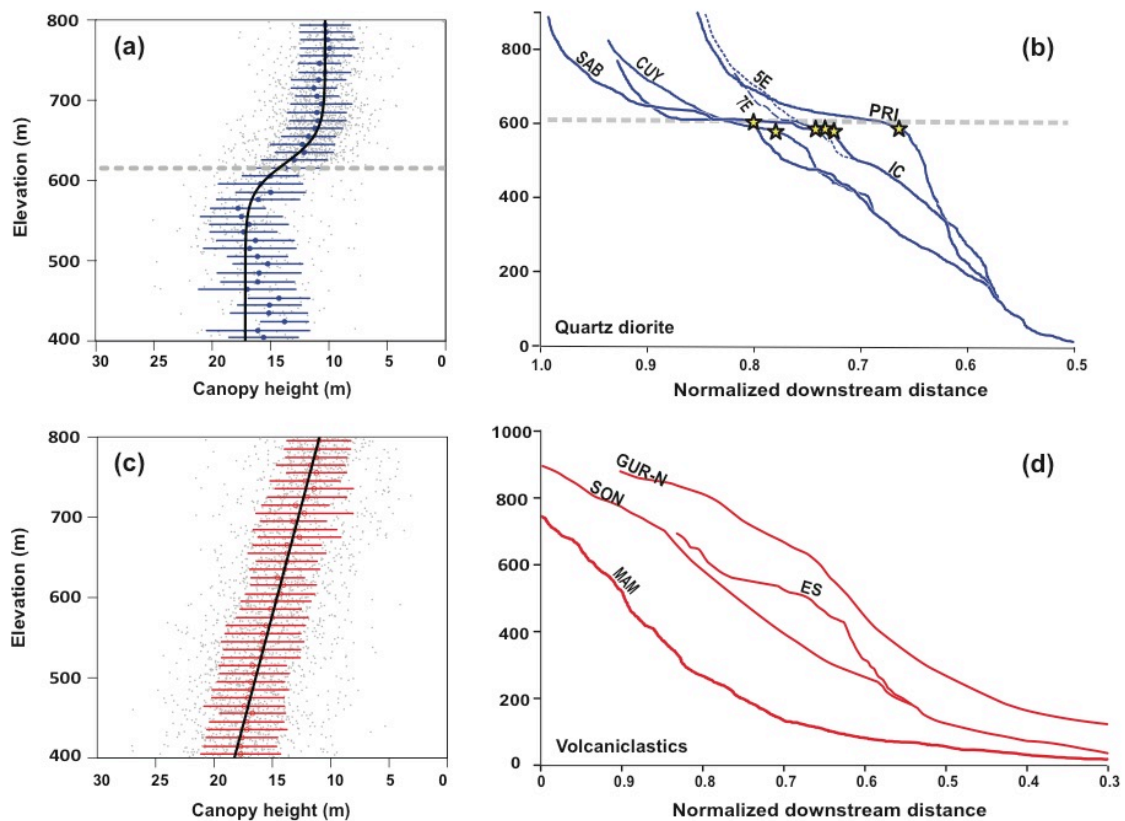
$$H = \frac{1}{1 + e^{k(x-x_0)}} \times m + b, \quad (1)$$

160 where k is a rate parameter, x_0 is the elevation where the inflection point in the height-elevation
 161 relationship occurs, while both m and b are scaling factors. We considered models with common
 162 parameters for both bedrock types and models with separate bedrock parameters. We also
 163 considered models with separate functional forms for the two bedrocks. Model fit was evaluated with
 164 Akaike Information Criteria (AIC) with no corrections for sample size because samples sizes were
 165 large (e.g. min. N = 1631 ha on quartz diorite). We used least-squares fits for linear and quadratic
 166 models, which result in maximum likelihood estimates. The sigmoid model was fit by maximum
 167 likelihood using simulated annealing. The optimization procedure was run 1,000 times from a
 168 random selection of different starting parameters.

169 3. Results

170 Abrupt changes in stand-level forest height occur on the quartz diorite bedrock but not on
 171 volcanoclastic bedrock (Fig. 2, Table 1). Models with separate parameters describe forest height-
 172 elevation responses across the two bedrock types far better than models with the same parameters
 173 for each bedrock type (Table A1-A2). Bedrock-specific parameters using the same functional form

174 provided worse fits to the data than using separate functional forms for each bedrock type (Table
 175 A2). The best-fit model included a sigmoidal functional form for quartz diorite bedrock and either
 176 linear (AIC = 19407.06) or quadratic functional forms for volcaniclastic bedrock (AIC = 19405.23).
 177 Because ΔAIC was small (e.g. < 2) between the two best fit models while ΔAIC was at least > 100 for
 178 all other model contrasts (Table A2), there is strong evidence for different functional forms
 179 characterizing forest height changes with elevation on quartz diorite relative to volcaniclastic
 180 bedrock. At the stand-level, rates of change in forest height with elevation were abrupt on quartz
 181 diorite near the knickpoints elevation ($k_{QD} = -0.0539 \pm 0.0056$, $x_{0QD} = 621.8 \pm 2.142$ m; Table 1). The
 182 decline in forest height happened over a narrow range of elevations (< 100 m) on the quartz diorite
 183 terrain. The inflection point occurred near the elevation of the pronounced knickpoints. On
 184 volcaniclastic bedrock, forest height decreased by -0.0182 ± 0.0006 m/m using the linear model (Table
 185 1). Appendix A includes summaries of all other height-elevation models that were tested (Tables A3-
 186 A11).
 187



188 **Figure 1.** Forest height – elevation patterns are best described using different functional forms for
 189 quartz diorite and volcaniclastic bedrock types. (a) Sigmoid model of forest height and elevation with
 190 inflection point located at 621.8 ± 2.142 m (mean \pm S.E.) near the elevation of the (b) knickpoints in
 191 stream profiles. Stars show the location of the knickpoints. (c) A line approximates the forest height -
 192 elevation pattern over the same elevation range on volcaniclastics where (d) knickpoints are absent
 193 from stream profiles. Within (a) and (c) points indicate means and lines indicate S.D. within 10 m
 194 elevation intervals.

195
 196
 197

198

199
200
201
202

Table 1. Model of forest height against elevation. Height-elevation was modeled using a scaled logistic function on quartz diorite (QD) and a linear model on volcanoclastic (VC) bedrock. The model is for the elevation interval between 400 m and 800 m (AIC = 19407.06). All estimates are significant at $P < 0.0001$ based on z-scores.

Parameter	Estimate	S.E.
L_{QD}	6.805	0.1566
k_{QD}	-0.0539	0.0056
x_{0QD}	621.8	2.142
b_{QD}	10.31	0.1093
β_{0VC}	25.54	0.3350
β_{1VC}	-0.0182	0.0006

203 4. Discussion

204 4.1. Aims revisited

205 We set out to test whether there were changes in forest height that occur as a result of the
206 tectonic uplift and erosional patterns across a mountain range, to gain insights into the processes
207 that influence vegetation patterns on a tropical elevation gradient. What we found is that forest
208 height changes abruptly near the elevation of knickpoints that demarkate portions of the elevation
209 gradient where erosion rates are high (e.g. lower elevations) from portions of the elevation gradient
210 where erosion rates are low (e.g. higher elevations) on the quartz diorite bedrock type. We also
211 compared results from the quartz diorite bedrock where erosion rates have been measured directly
212 using cosmogenic isotopes and where pronounced knickpoints are present, to the bedrock without
213 directly measured erosion rates, but that lacks the knickpoints. Our results show that on the
214 bedrock without the pronounced knickpoints, presumably where there are not sharp changes in
215 erosion rates occurring over similar elevations, the forest height – elevation patterns are well
216 approximated as linear. Forest height on the quartz diorite could vary abruptly due to sharp
217 decreases in productivity without a change in species composition or may result from abrupt
218 changes in species composition.

219 4.2. General Importance

220 These findings may have general importance for understanding vegetation patterns in mountain
221 ranges. Climate is often viewed as the primary driver of vegetation patterns in mountains and
222 elevation gradients are correctly assumed to be climate gradients [1]. Nevertheless, elevation
223 gradients are also edaphic gradients, in part due to climate, but also due to geological reasons,
224 including spatial variation in bedrock types [13-14], but also due to the land surface dynamics that
225 depend on tectonics and erosion. Soil variation is generally important to understanding vegetation
226 patterns in tropical forests [15-18], but the role of soils along elevation gradients is not well
227 understood.

228 One of the most general patterns in biogeography is the mass-elevation effect [19-20] where rates
229 of change in forest properties vary as a function of mountain size and proximity to other mountains
230 or large water bodies. Large mountains have slower rates of change in forest properties than do
231 smaller mountains. Hypotheses to explain the mass-elevation effect fall into two categories: (1)
232 direct climate hypotheses and (2) indirect climate hypotheses. The primary indirect climate
233 hypothesis is that increasing cloud cover at lower elevations in small mountains near large water
234 bodies results in decreased rates of organic matter mineralization in soils, thereby decreasing rates of
235 nutrient cycling and nutrient supply for plants, with plant productivity and species distributions
236 along elevation gradients limited by nutrient availability. These hypotheses have been difficult to
237 test, but we suggest that using natural experiments where geological factors cause variation in soil

238 nutrient availability could provide important insights into understanding the role of bottom-up
239 controls on phenomena such as the mass-elevation effect.

240 5. Conclusions

241 The geological processes that build and deconstruct mountains play a prominent role in spatial
242 patterns of vegetation in relation to elevation in the Luquillo Mountains.

243 **Supplementary Materials:** The following are available online at www.mdpi.com/link, Supplementary Results.

244 **Acknowledgments:** This is collaborative research between the Luquillo Critical Zone Observatory and Luquillo
245 Long-Term Ecological Research site. This work was supported by National Science Foundation grants DEB-
246 1546686, EAR-0722476, and EAR-0922307.

247 **Author Contributions:** All authors conceived and designed the research; J.A.W. performed the research; J.A.W.
248 analyzed the data; All authors contributed reagents/materials/tools; J.A.W. and G.B. wrote the paper. All authors
249 commented on drafts the paper and approved the paper.

250 **Conflicts of Interest:** The authors declare no conflict of interest.

251 References

- 252 1. Mahli, Y.; Silman, M.; Salinas, N.; Bush, M.; Saachi, S. Introduction: Elevation gradients in the tropics:
253 laboratories for ecosystem ecology and global change research. *Global Change Biology* **2010** *16*, 3171-3175.
- 254 2. Duque, A.; Stevenson, P.R.; Feeley, K. J. Thermophilization of adult and juvenile tree communities in the
255 northern tropical Andes. *Proceedings of the National Academy of Sciences USA* **2015** *112*, 10744-10749.
- 256 3. Morueta-Holme, N.; Engemann, K.; Sandoval-Acuña, P.; Jonas, J.D.; Segnitz, R.M.; Svenning, J.C.. Strong
257 upslope shifts in Chimborazo's vegetation over two centuries since Humbolt. *Proceedings of the National*
258 *Academy of Sciences USA* **2015** *112*, 12741-12745.
- 259 4. Hahm, W. J.; Riebe, C.S; Lukens, C.E.; Araki, S. Bedrock composition regulates mountain ecosystems and
260 landscape evolution. *Proceedings of the National Academy of Sciences USA* **2014** *111*, 3338-3343.
- 261 5. Milodowski, D.T.; Mudd, S.M.; Mitchard, E.T.A. Erosion rates as a potential bottom-up control of forest
262 structural characteristics in the Sierra Nevada Mountains. *Ecology*. **2015** *96*, 31-38.
- 263 6. Brocard, G. Y.; Willenbring, J.K.; Scatena, F.N.; Johnson, A.H. Effects of a tectonically-triggered wave of
264 incision on riverine exports and soil mineralogy in the Luquillo Mountains of Puerto Rico. *Appl. Geochem.*
265 **2015** *63*, 586-598.
- 266 7. Brocard, G. Y., J. K. Willenbring, T. Miller, and F.N. Scatena. Resilience of a transport-limited relict
267 landscape to dissection by upstream migrating knickpoints. *Journal of Geophysical Research Earth*
268 *Surface* **2016**, doi: 10.1002/2015JF003678.
- 269 8. Lefsky, M.A.; Cohen, W.B.; Parker, G.G.; Harding, D.J. Lidar remote sensing for ecosystem studies.
270 *Bioscience* **2002** *52*, 19-30.
- 271 9. Asner, G.P.; Mascaro, J. Mapping tropical forest carbon: Calibrating plot estimates to a single lidar metric.
272 *Remote Sensing of Environment* **2014** *140*, 614-624.
- 273 10. Skidmore, A.K.; Pettorelli, N.; Coops, N.C.; Geller, G.N., Hansen, M.; et al. Environmental science: agree
274 on biodiversity metrics to track from space. *Nature* **2015** *523*, 403-405. doi: 10.1038/523403a.
- 275 11. ten Brink, U. Vertical motions of the Puerto Rico Trench and Puerto Rico and their cause. *Journal of*
276 *Geophysical Research* **2005** *110*, B06404. doi: 10.1029/2004JB003459.
- 277 12. Porder, S.; Johnson, A. H.; Xing Xing, H.; Brocard, G.; Goldsmith, S.; Pett-Ridge, J. Linking geomorphology,
278 weathering and cation availability in the Luquillo Mountains of Puerto Rico. *Geoderma* **2015** *249-250*, 100-
279 110. doi: 10.1016/j.geoderma.2015.03.002.
- 280 13. Kitayama, K.; Aiba, S. Ecosystem structure and productivity of tropical rain forests along altitudinal
281 gradients with contrasting soil phosphorus pools on Mount Kinabalu, Borneo. *Journal of Ecology* **2002** *90*,
282 37-51.
- 283 14. Aiba, S.; Kitayama, K. Structure, composition and species diversity in an altitude substrate matrix of rain
284 forest tree communities on Mount Kinabalu, Borneo. *Plant Ecology* **1999** *140*, 139-157.
- 285 15. Fine, P.V.A.; Mesones, I.; Coley, P.D. Herbivores promote habitat specialization by trees in Amazonian
286 forests. *Science* **2004** *305*, 663-665.

- 287 16. Vitousek, P.; Asner, G.P.; Chadwick, O.A.; Hotchkiss, S. Landscape-scale variation in forest structure and
288 biogeochemistry across a substrate age gradient in Hawaii. *Ecology* **2009** *90*, 3074-3086.
- 289 17. Higgins, M.A.; Ruokolainen, K.; Tuomisto, H.; Llerena, N.; Cardenas, G.; et al. Geological control of floristic
290 composition in Amazonian forests. *J. Biogeogr.* **2011** *38*, 2136-2149.
- 291 18. Condit, R.; Englebrecht, B.M.J.; Pino, D.; Pérez, R.; Turner, B.L. Species distributions in response to
292 individual soil nutrients and seasonal drought across a community of tropical trees. *Proc. Natl. Acad. Sci.*
293 *USA* **2013** *110*, 5064-5068.
- 294 19. Grubb, P.J. Interpretation of the 'Massenerhebung' effect on tropical mountains. *Nature* **1971** *229*, 44-45.
- 295 20. Grubb, P.J. Control of forest growth and distribution on wet tropical mountains: with special reference to
296 mineral nutrition. *Annual Reviews of Ecology and Systematics* **1977** *8*, 83-107.



© 2016 by the authors. Submitted for possible open access publication under the terms and conditions of the Creative Commons Attribution (CC-BY) license (<http://creativecommons.org/licenses/by/4.0/>).